

# CFD 3 Assignment 2

Mustafa Sabri Güverte, 4548361

April 1, 2021

# 1 — Determining Viscosity

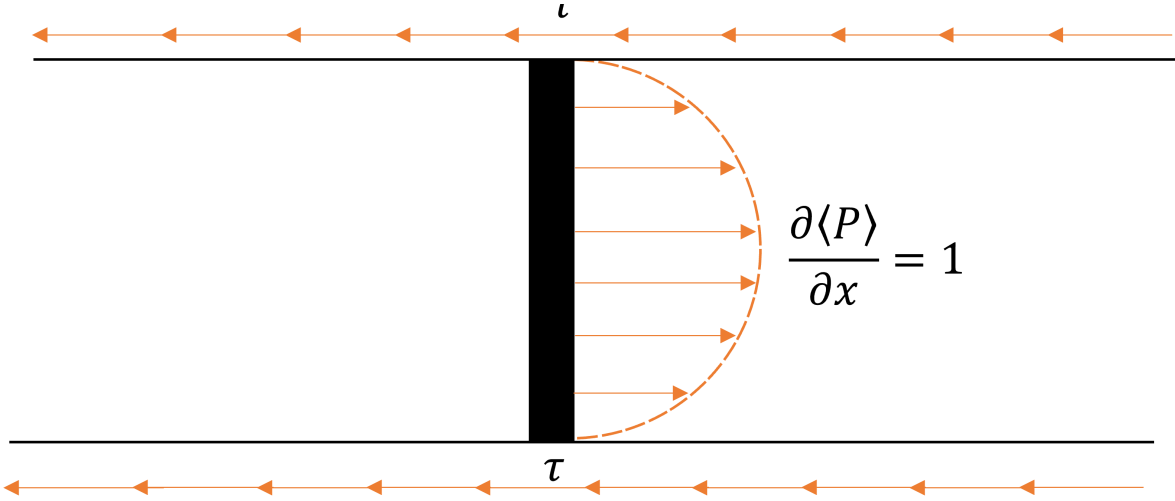


Figure 1.1: Freebody Diagram

In 1.1, one can make a balance of forces using the knowledge that:

$$\int_0^x P dx = \int_0^x \tau dx = F_{net} \quad (1.1)$$

$$\int_0^L \frac{d \langle P \rangle}{dx} dx = P \quad (1.2)$$

Giving us the overall balance

$$\int_0^{2h} \int_0^L \frac{d \langle P \rangle}{dx} dx dy = \int_0^L \tau dx + \int_0^L \tau dx \quad (1.3)$$

$$\int_0^{2h} \int_0^L 1 dx dy = \int_0^L \tau dx + \int_0^L \tau dx \quad (1.4)$$

$$2hL = 2\tau L \quad (1.5)$$

$$h = \tau \quad (1.6)$$

Now considering:

$$u_\tau = \sqrt{\frac{\tau_{wall}}{\rho}} = 1 \quad (1.7)$$

$$Re_\tau = \frac{u_\tau h}{v} = \frac{u_\tau}{v} \quad (1.8)$$

Giving us that

$$\nu = \frac{1}{Re} \quad (1.9)$$

## 2 — Analysing Different Cases

Looking at the different cases, one can make striking observation. Firstly, it is evident that all cases perform more successfully (Proportionally closer to DNS) for  $U_{mean}$  and  $w_{rms}$  than  $u_{rms}$  and  $v_{rms}$ . One also notices for most scenarios, all cases have a constant deviation from the DNS solution.

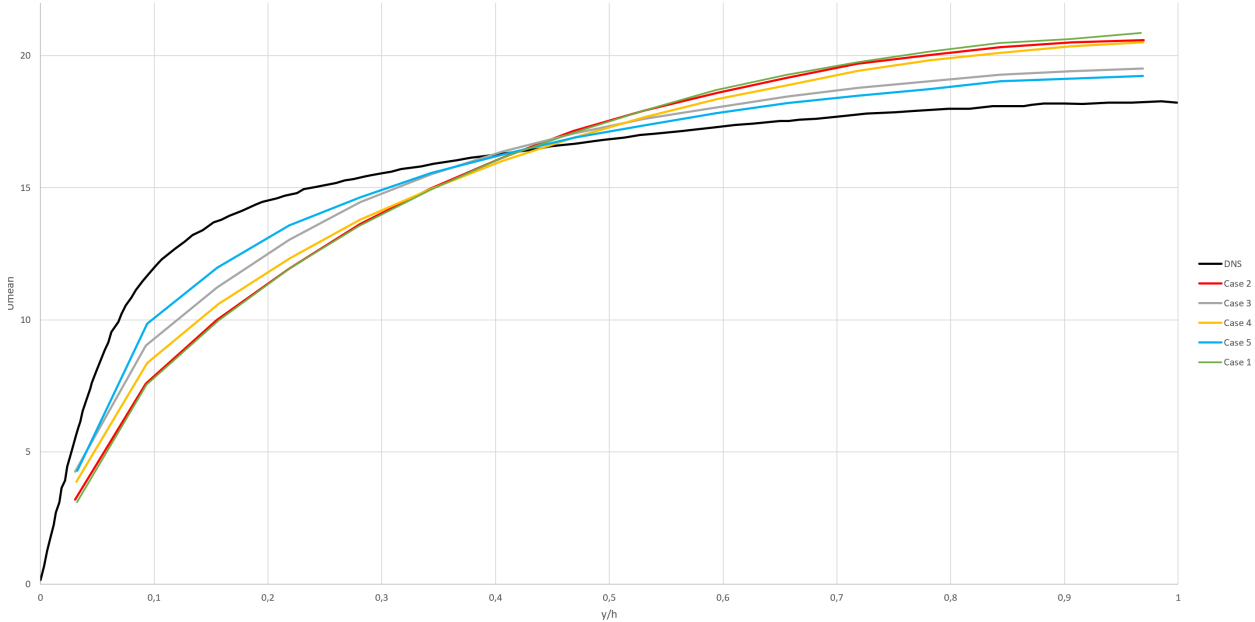


Figure 2.1: Umean for all cases

For  $U_{mean}$ , cases two and one have almost twice the relative distance from the DNS simulation with respect to case five. One observes that at a certain value of  $y/h$  all cases intersect the DNS solution. Before and after the simulation the cases diverge from the DNS solution.

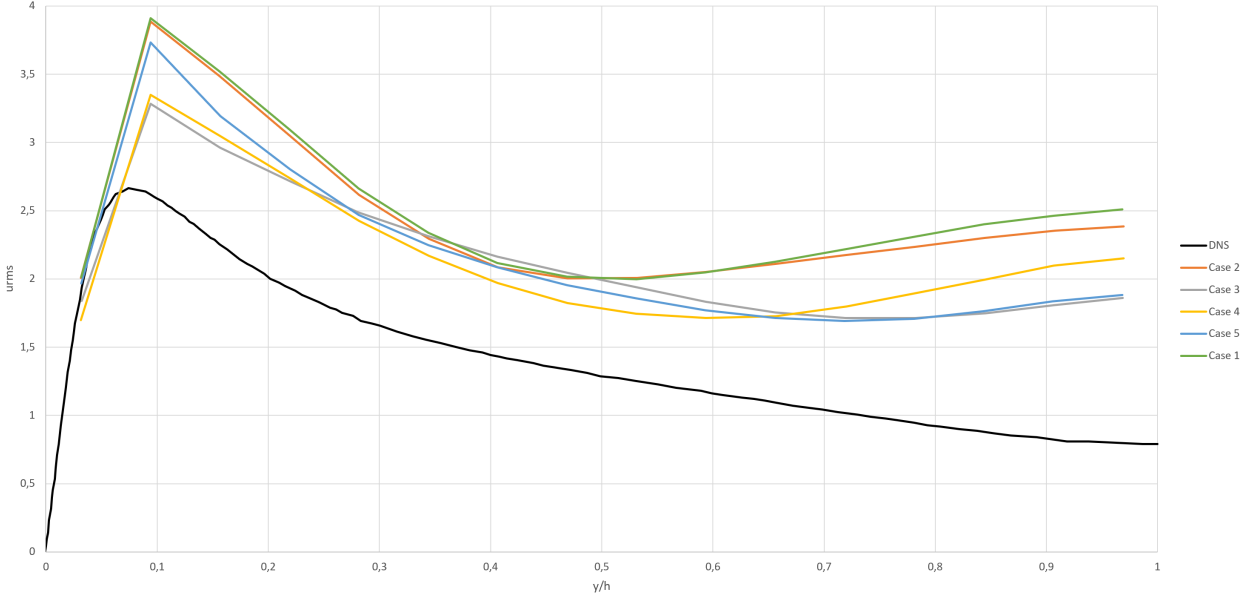


Figure 2.2: urms for all cases

For  $u_{rms}$ , one observes less pronounced performance differences, however the obvious worst performer is case one, followed by case two then case four. That being said, initially for  $y/h$  less than 0.65, case four actually seems to perform the best. Case three and five perform almost equally either rival case four or beat it in terms of accuracy.

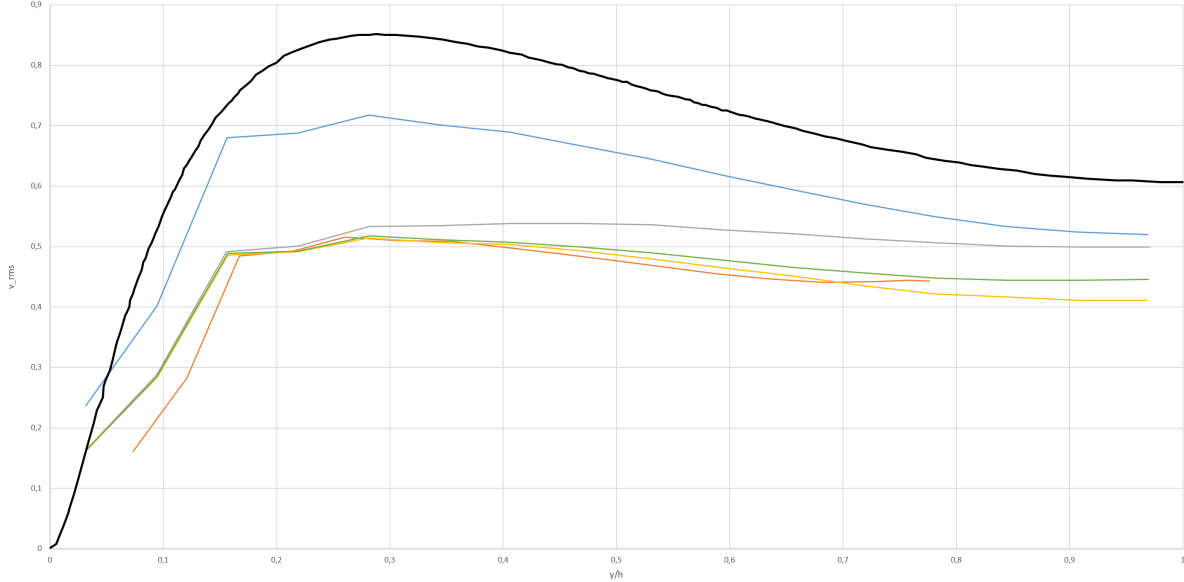


Figure 2.3: vrms for all cases

For  $v_{rms}$ , it is obvious case five performs the best followed by case three then case one then case two and four performing almost equally bad, it is interesting to note that case one two three and four perform identically until  $y/h$  less than 0.25 and only then slight divergences happen, case five however, is not only the most distinct case in terms of performance it consistently has a lead to the other cases up until the end.

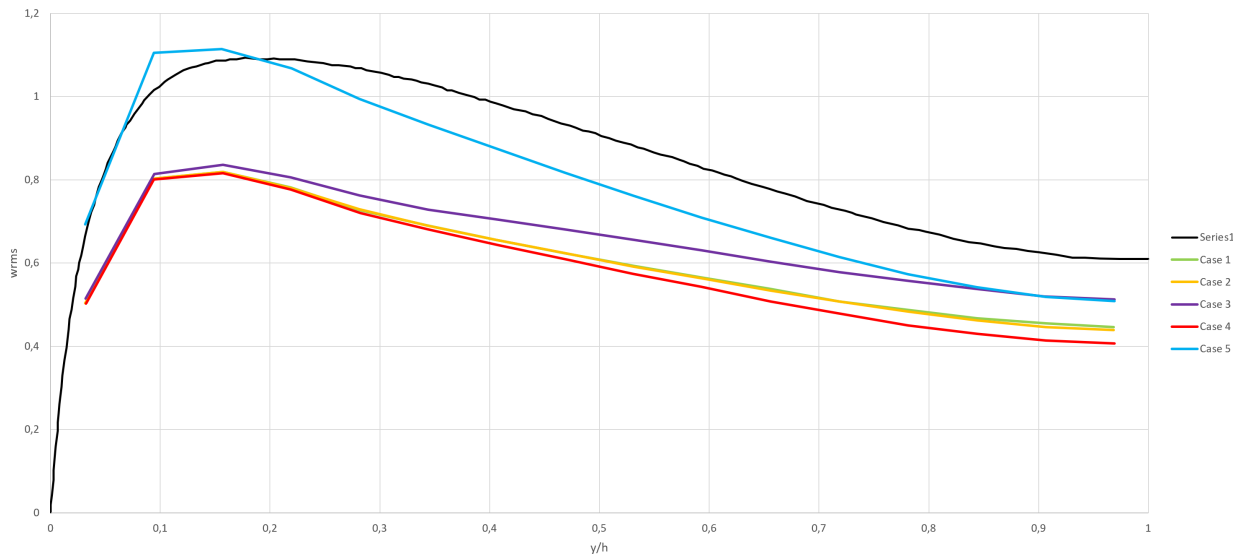


Figure 2.4: wrms for all cases

For  $w_{rms}$ , one observes the clear best performer to be case five, the other cases perform almost equally as bad bar case three which converges with case five to be the best performing case (only after  $y/h$  is greater than 0.85).

### **3 — Case choice for 64 case**

It is evident in almost all scenarios, that case five is the best performing case with the least deviance from the DNS among most scenarios. Hence it has been chosen for

## 4 — Reynold Calculation

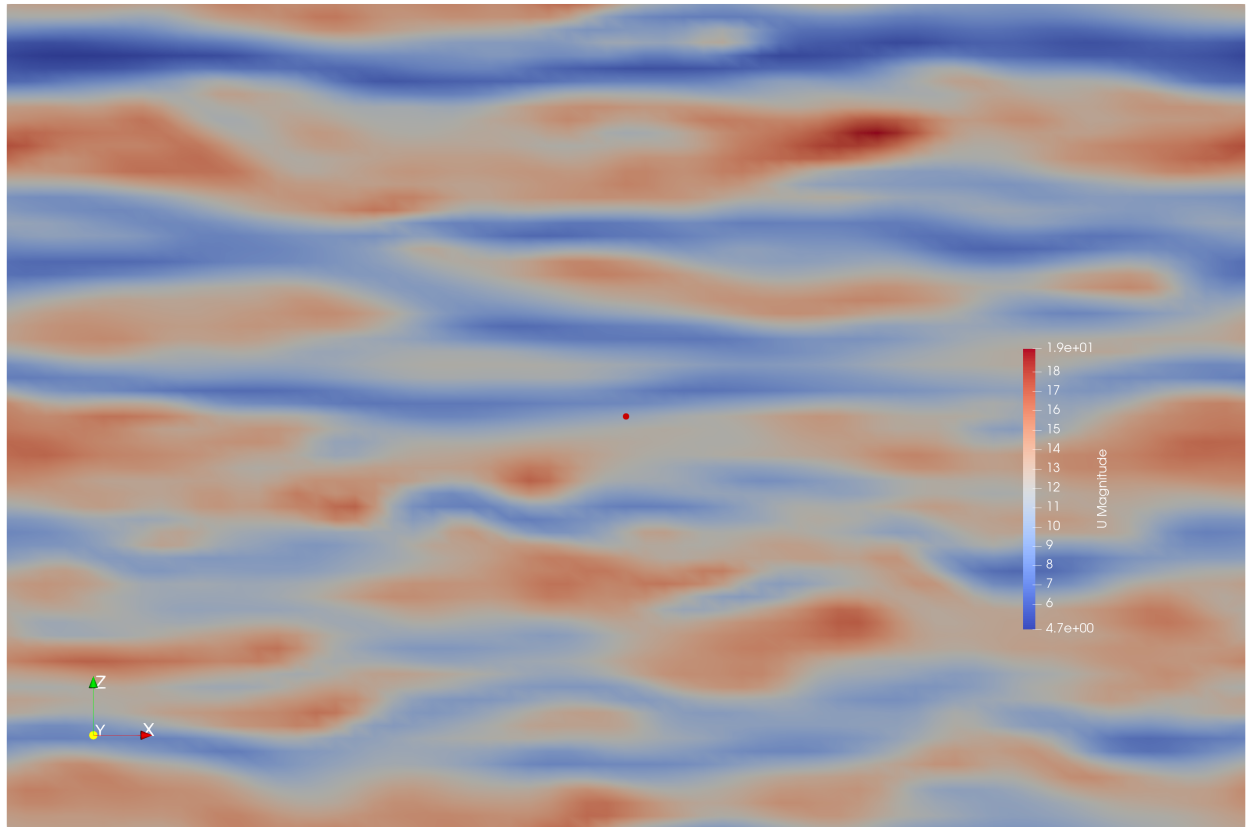


Figure 4.1: U magnitude at  $y = 0.1$

Average streak height is found to be  $h = 0.4525$  giving us a Re of:

$$Re = \frac{1}{\frac{h}{z^+ = 100}} = 220.99 \quad (4.1)$$

$$5 \quad - \quad \nu_{sgs}$$

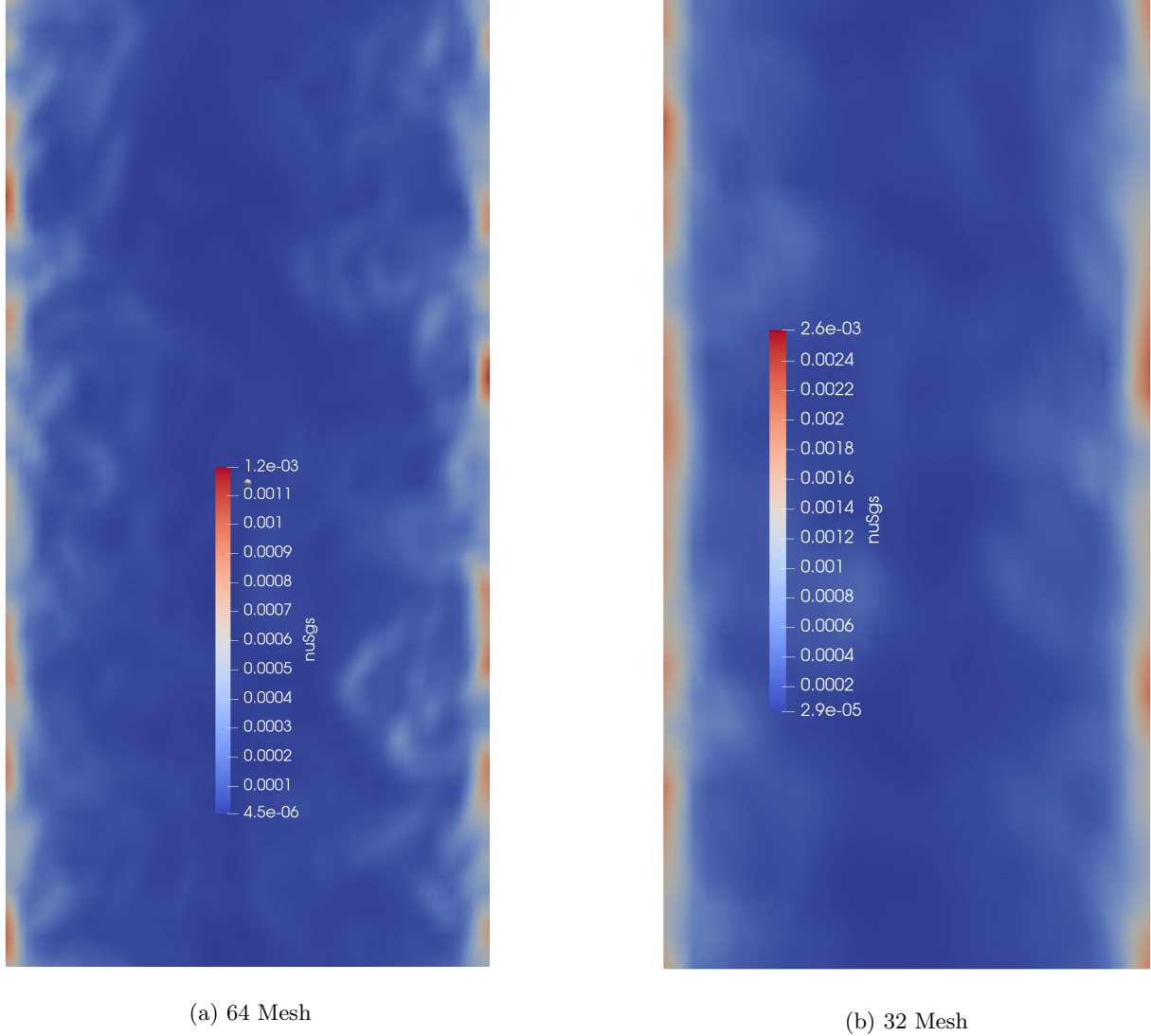


Figure 5.1: Comparison of Meshes

One observes maximum viscosity occurs at either the top or bottom bounds of the channel (left and right bounds of the charts). Both meshes have very similar shapes and characteristics with the exception that the 64 mesh has a smaller  $\nu_{sgs}$  magnitude and seems more concentrated around certain locations at the boundary, in comparison to the 32 mesh that in general spreads around the boundary more.

$\nu_{sgs}$  is dependent on the following:

$$S_{ij} = \frac{1}{2} \left( \frac{\partial \bar{u}_i}{\partial x_j} + \frac{\partial \bar{u}_j}{\partial x_i} \right) \quad (5.1)$$

[2]

A less refined mesh has larger values of  $\frac{\partial \bar{u}_i}{\partial x_j}$  and  $\frac{\partial \bar{u}_j}{\partial x_i}$  thus larger magnitudes for  $\nu_{sgs}$ . Furthermore having coarser grid also means that local maxima diverge more and thus spread out over more of the boundary compared to a refined grid.

## 6 — Piomelli's Shift

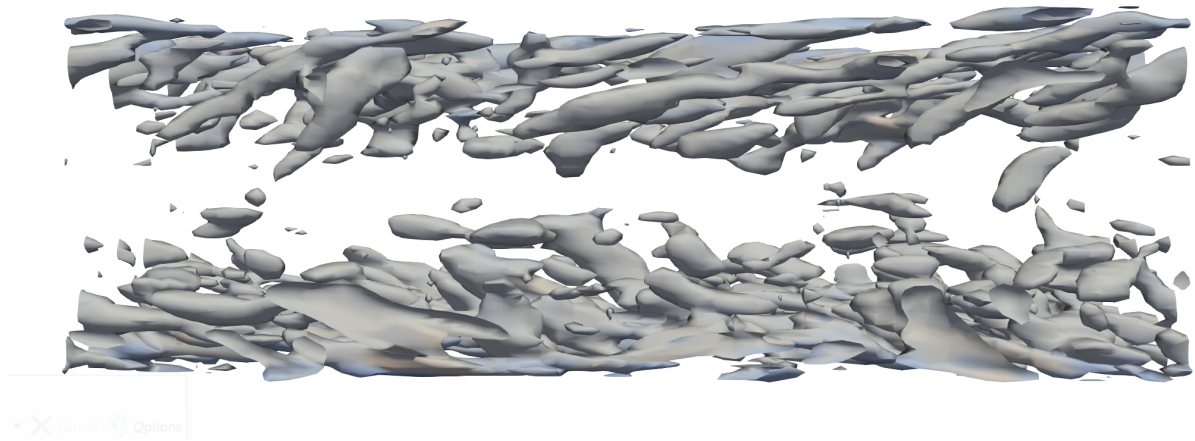


Figure 6.1:  $Q = 100$

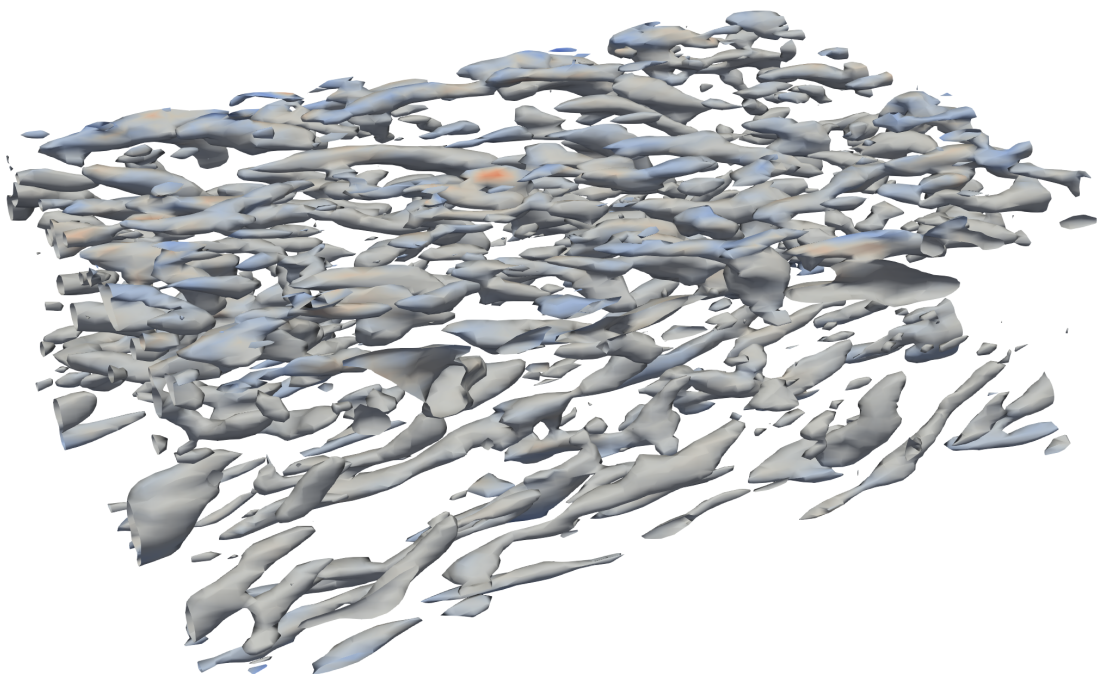


Figure 6.2:  $Q = 100$

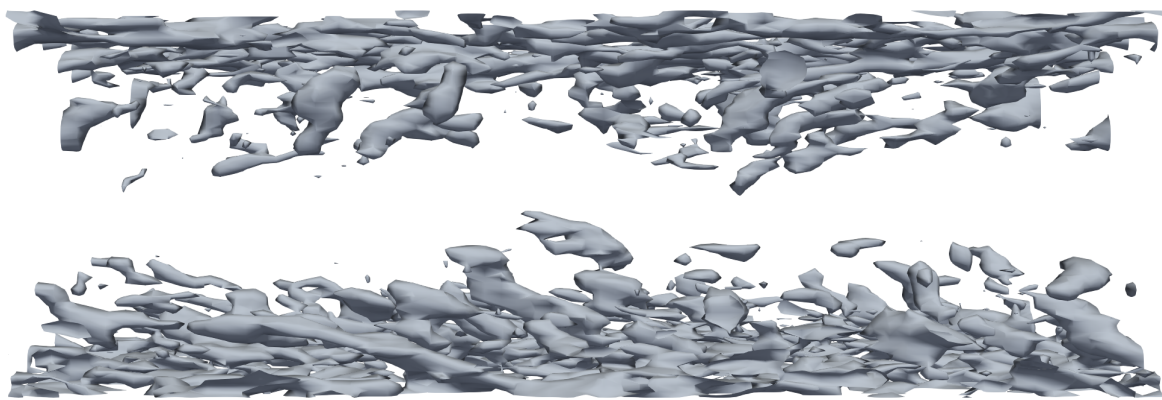


Figure 6.3:  $\lambda = -100$

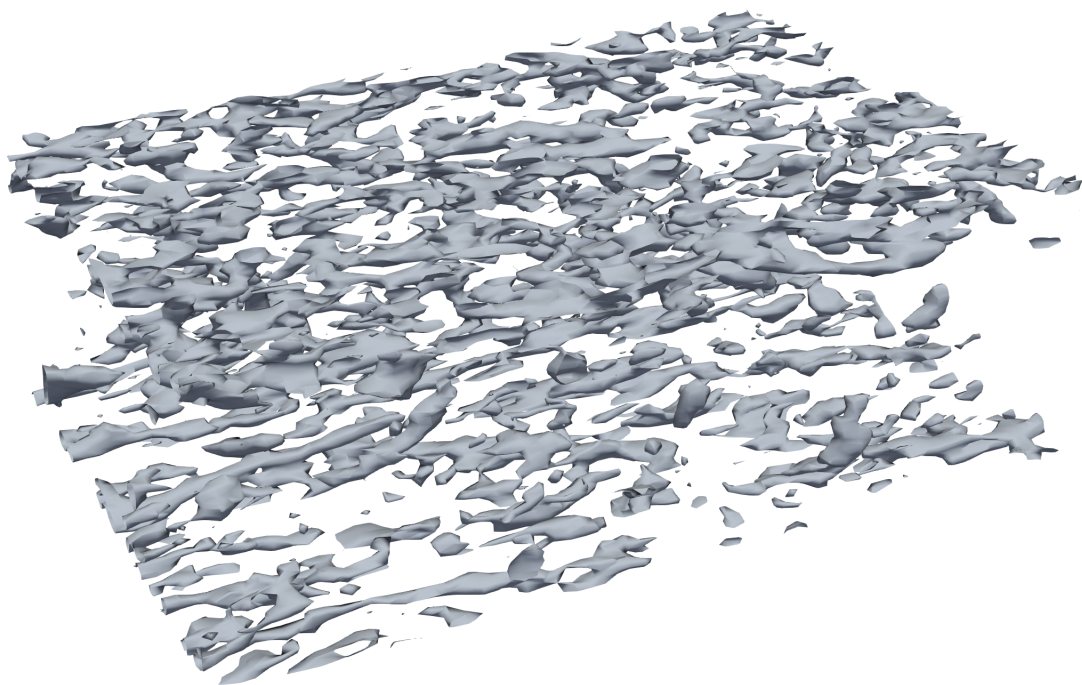


Figure 6.4:  $\lambda = -100$

Piomelli's shift is given by:

$$\Delta_s = (1 - |y_2|) \cot(\alpha^\circ) \quad (6.1)$$

Where  $\alpha$  is 8 for  $y^+ = 50$  and 13 for  $y^+ = 100$  [2]. Giving us  $\Delta_{s50} = -348.65$  and  $\Delta_{s100} = -428.82$ .

## 7 — Searching for Hairpin Vortices

After having looked at the 64 grid for each timestep for the given lambda and Q values, no hairpin vortices were visible. Hairpin vortices are distinctly shaped after their namesake and come in clusters which was not a phenomena observed for either case at any time frame. Certain sections of the flow resemble quasi-hairpinlike shapes however these are not distinct enough, or not clustered to consider them hairpin vortices. After having researched further into hairpin vortices, it is stated that hairpin vortices can be found even in laminar flows thus the Reynolds number is most likely not the reasoning. What is stated is that in turbulent boundary layers completely symmetric hairpin vortices are hardly ever found and more often one observes distorted structures such as one legged hairpins [3]. This source along with other support the finding of potentially quasi-symmetric hairpin vortices. Further simulations, reaching Reynolds up to 4300 (much larger than ours) still does not observe any hairpin vortices in their respective studies giving credence to the inability to find hairpin vortices in our case [1].

# Bibliography

- [1] G. Eitel-Amor, R. Örlü, P. Schlatter, and O. Flores. Hairpin vortices in turbulent boundary layers. *Physics of Fluids*, 27(2):025108, 2015.
- [2] Ugo Piomelli, Joel Ferziger, Parviz Moin, and John Kim. New approximate boundary conditions for large eddy simulations of wall-bounded flows. *Physics of Fluids A: Fluid Dynamics*, 1(6):1061–1068, 1989.
- [3] H.A. Zondag. *The dynamics of hairpin vortices in a laminar boundary layer*. PhD thesis, Applied Physics, 1997.